Mn-rich tourmaline from Austria: structure, chemistry, optical spectra, and relations to synthetic solid solutions

ANDREAS ERTL,[1,*] JOHN M. HUGHES,[2] STEFAN PROWATKE,[3] GEORGE R. ROSSMAN,[4] DAVID LONDON,[5] AND ERIC A. FRITZ[6]

[1]Institut für Mineralogie und Kristallographie, Geozentrum, Universität Wien, Althanstrasse 14, A-1090 Vienna, Austria
[2]Department of Geology, Miami University, Oxford, Ohio 45056, U.S.A.
[3]Mineralogisches Institut, Universität Heidelberg, Im Neuenheimer Feld 236, D-69120 Heidelberg, Germany
[4]Division of Geological and Planetary Sciences, California Institute of Technology, Pasadena, California 91125-2500, U.S.A.
[5]School of Geology and Geophysics, University of Oklahoma, 100 East Boyd Street, Room 810 SEC, Norman, Oklahoma 73019, U.S.A.
[6]3541 Paseo de Francisco no. 240, Oceanside, California 92056, U.S.A.

ABSTRACT

Yellow-brown to pink Mn-rich tourmalines with MnO contents in the range 8–9 wt% MnO (~0.1 wt% FeO) from a recently discovered locality in Austria, near Eibenstein an der Thaya (Lower Austria), have been characterized by crystal structure determination, by chemical analyses (EMPA, SIMS), and by optical absorption spectroscopy. Qualitatively, the optical spectra show that Mn^{2+} is present in all regions of the crystals, and that there is more Mn^{3+} in the pink regions (~8% of the total Mn is Mn^{3+}) than in the yellow-brown regions. A gamma-ray irradiated crystal fragment is distinctly pink compared to the yellow-brown color of the sample before irradiation, but it still has hints of the yellow-brown color, which suggests that the natural pink color in Mn-rich tourmaline from this locality is due to natural irradiation of the initial Mn^{2+}. For these Mn-rich and Li-bearing olenite samples, crystal structure refinements in combination with the chemical analyses give the optimized formulae $^X(Na_{0.80}Ca_{0.01}\square_{0.19})$ $^Y(Al_{1.28}Mn^{2+}_{1.21}Li_{0.37}Fe^{2+}_{0.02}\square_{0.12})$ $^ZAl_6$ $^T(Si_{5.80}Al_{0.20})$ B_3O_{27} $[(OH)_{3.25}F_{0.43}O_{0.32}]$, with a = 15.9466(3) Å, c = 7.1384(3) Å, and R = 0.036 for the sample with ~9 wt% MnO, and $^X(Na_{0.77}Ca_{0.03}\square_{0.20})$ $^Y(Al_{1.23}Mn^{2+}_{1.14}Li_{0.48}Fe^{2+}_{0.02}Ti_{0.01}\square_{0.12})^ZAl_6{}^T(Si_{5.83}Al_{0.17})$ B_3O_{27} $[(OH)_{3.33}F_{0.48}O_{0.19}]$ for a sample with a = 15.941(1) Å, c = 7.136(1) Å, R = 0.025 and ~8 wt% MnO. The refinements show 1.22–1.25 Al at the Y site. As the Mn content increases, the Li and the F contents decrease. The Li content (0.37–0.48 apfu) is similar to, or lower than, the Li content of olenite (rim-composition) from the type locality, but these Mn-rich tourmalines do not contain $^{[4]}B$. Like the tourmaline from Eibenstein an der Thaya, synthetic Mn-rich tourmaline (in a Li + Mn-bearing system), containing up to ~0.9 apfu Mn (~6.4 wt% MnO), is aluminous but not Li-rich. This study demonstrates that although a positive correlation exists between Mn and Li (elbaite) in tourmaline samples from some localities, this coupling is not required to promote compatibility of Mn in tourmaline. The a parameter in Mn-rich tourmalines (MnO: ≥3 wt%) is largely a function of the cation occupancy of the Y site (r^2 = 0.97).

INTRODUCTHON

Mn-rich tourmaline has been described from several localities. Kunitz (1929) reported an Mn-rich tourmaline from Nertschinsk, USSR, with 8.21 wt% MnO as "tsilaisite" [Kunitz proffered the hypothetical endmember formula $NaMn^{2+}_3Al_6(Si_6O_{18})(BO_3)_3(OH)_4$]. The name was derived from the Tsilaisina locality in Madagascar, described by Duparc et al. (1913). Schmetzer and Bank (1984) and Rossman and Mattson (1986) reported MnO contents up to 6.85 wt% (FeO below detection limit) in yellow tourmaline samples from ca. 150 km north of Chipata, Zambia. Prior to this work, the most Mn-rich tourmaline (8.86 wt% MnO) was described by Shigley et al. (1986) from an unknown locality (Zambia?). Morgan and London (1999) characterized compositional variations in tourmaline from the Little Three pegmatite, Ramona, California, in which the MnO content reached 6.68 wt% in the most evolved

tourmaline found in miarolitic cavities. Recently, Novák (2000) published tourmaline compositions from the zoned elbaite pegmatite at Pikárec, Czech Republic, with up to 7.93 wt% MnO and 0.67 wt% FeO. All these samples have Na dominant over Ca and vacancies at the X site.

Nuber and Schmetzer (1984) determined the crystal structure of a yellow Mn-rich tourmaline (from Zambia, with MnO = 6.72 wt%, FeO = 0.05 wt%) with the approximate composition $(Na_{0.85}Ca_{0.04}\square_{0.11})$ $(Al_{1.53}Mn_{0.93}Li_{0.42}Ti_{0.04}Fe_{0.01}\square_{0.07})$ $Al_{6.00}$ $(BO_3)_3$ $(Si_{5.98}O_{18})$ $[(OH)_{2.63}O_{0.37}]$ $[F_{0.48}O_{0.52}]$ (chemical analysis by Schmetzer and Bank 1984; Ti has been assigned to the Y site). The lattice constants of this tourmaline sample were given as a = 15.916(3), c = 7.130(1) Å. The authors refined an occupancy of 1.066(6) Al at the Y site (R = 3.0 %). Burns et al. (1994) described the crystal structures of eight Mn-bearing to Mn-rich tourmalines with MnO contents in the range 0.35–6.23 wt% (R = 1.8–2.5 %).

Tourmaline, highly enriched in Mn (up to 8.89 wt% MnO), was recently found in a Variscan topaz- and cassiterite-bearing

---

pegmatite near Eibenstein an der Thaya, Lower Austria (Ertl et al. in preparation). Those authors report an increasing Mn content from the center to the rim of the samples, and describe the associated minerals including their chemical compositions. This study focuses on the crystal structure of this unusually Mn-rich tourmaline from Austria, with MnO contents in the range 8–9 wt%, and on the relationships between tourmaline structure and chemistry.

EXPERIMENTAL DETAILS

Eleven small fragments were taken from the rims of three yellow-brown to pink Mn-rich tourmaline samples. The structures of these eleven fragments were refined using the methods described below. The two samples with the highest refined electron occupancy (suggesting the highest Mn content) at the Y site, combined with the largest lattice parameters, are described in this study (samples BT and P6).

Crystals BT (~50 μm in diameter) and P6 (~100 μm in diameter) were mounted on a Bruker Apex CCD diffractometer equipped with graphite-monochromated MoKα radiation. Redundant data were collected for an approximate sphere of reciprocal space, and were integrated and corrected for Lorentz and polarization factors using the Bruker program SaintPlus (Bruker AXS Inc. 2001).

The structures were refined using tourmaline starting models and the Bruker SHELXTL v. 6.10 package of programs, with neutral-atom scattering factors and terms for anomalous dispersion. Refinement was performed with anisotropic thermal parameters for all non-hydrogen atoms. Table 1 offers crystal data and details of structure refinement for the two tourmalines.

The two crystals selected for crystal structure determination were prepared for chemical analysis. All elements except B, Li, Be, and H were determined with a Cameca SX51 electron microprobe (EMP) equipped with five wavelength-dispersive spectrometers (University of Heidelberg). Operating conditions were 15 kV accelerating voltage, 20 nA beam current, and a beam diameter of 5 μm. Na was the first element which was analyzed on the spectrometer and assays have proved that counting was stable with increasing time. Peaks for all elements were measured for 10 s, except for Mg (20 s), Cr (20 s), Ti (20 s), Zn (30 s), Cl (30 s), and F (40 s). The fluorine Kα line interferes with the Fe and MnLα lines, requiring a correction for the measured F values [F = F_{meas} − (−0.000055 FeO^2 + 0.0889 FeO − 0.0044) + 0.015 MnO; Kalt et al. 2001]. We used the following (natural and synthetic) standards and X-ray lines for calibration: albite (NaKα), periclase (MgKα), corundum (AlKα), wollastonite (SiKα), rutile (TiKα), eskolaite (CrKα), scapolite (ClKα), orthoclase (KKα), wollastonite (CaKα), hematite (FeKα), rhodonite (MnKα), gahnite (ZnKα), and topaz (FKα). The analytical data were reduced and corrected using the PAP routine. For tourmaline, a modified matrix correction was applied assuming stoichiometric O atoms and all non-measured components as B_2O_3. The accuracy of the electron microprobe analyses of tourmaline and the correction procedure was checked by measuring three samples of reference tourmalines (98114: elbaite, 108796: dravite, 112566: schorl). Analyses of these tourmaline samples are pre-

sented in the context of an interlaboratory comparison study (Dyar et al. 1998, 2001). Coincidence between the published analyses and the measured values was satisfactory. Under the described conditions, analytical errors associated with all analyses are ±1% relative for major elements and 5% relative for minor elements.

H, Li, Be, and B were determined by secondary ion mass spectrometry (SIMS) with a CAMECA ims 3f ion microprobe. Primary ions were O-ions accelerated to 10 keV. An offset of 75 V was applied to the secondary accelerating voltage of 4.5 keV, so that secondary ions with an initial energy of 75 ± 20 eV were analyzed (energy filtering). This adjustment suppresses effects of light elements related to the structure of the matrix (Ottolini 1993). For B, Li, and Be the primary current was 5 nA, resulting in a sputtering surface ~15 μm in diameter. The spectrometer's mass resolution $M/\Delta M$ for B, Li, and Be was set to ~1100 (10%) to suppress interferences ($6LiH^+$, $10BH^+$, Al^{3+}). Secondary ions ^1H, ^7Li, ^9Be, and ^{11}B were collected with an ion-imaged field of 150 μm diameter.

For H the primary beam current was 10 nA and $M/\Delta M$ was set to ~400 (10%). To reduce the rate of contamination with water the primary beam was scanned over an area of 40 × 40 μm. By choosing a smaller field aperture, the analyzed area was restricted to 10 μm diameter in the center of the scanned area. This method reduces the effect of water contamination, which was found to be higher on the edge of the primary beam spot than in the center. Water contamination was further reduced using a cold trap cooled with liquid nitrogen attached to the sample chamber of the ims 3f. The count rates of the analyzed isotopes (^1H, ^7Li, ^9Be, and ^{11}B) were normalized to the count rate of ^{30}Si.

The relative ion yield (RIY) for B was determined using three different tourmalines: elbaite (98144), dravite (108796), and schorl (112566), described and analyzed by Dyar et al. (1998, 2001). The relative reproducibility (1σ) of the B analyses was <1%. Because of a substantial matrix effect during hydrogen-measurements (King et al. 2002) the RIY for H was determined using only the elbaite (98144) sample because its composition is similar to the composition of the analyzed Mn-olenite.

For Li and Be the reference material was NIST SRM 610 (Perkins et al. 1997). The relative reproducibility was <1% for Li and <5% for Be. The accuracy is limited by matrix effects and the uncertainty of the element concentrations in the reference material; the relative uncertainty is estimated to be <25% for H, <20% for Li and Be, and <10% for B.

A 1.5 × 0.8 mm crystal of manganian-olenite (NewBT) was prepared as a 0.245 mm thick parallel plate polished on both sides. Polarized optical absorption spectra in the 380–1100 nm range were obtained at about 1 nm resolution with a locally built microspectrometer system consisting of a 1024 element Si diode-array detector coupled to a grating spectrometer system via fiber optics to a highly modified NicPlan infrared microscope containing a calcite polarizer. Pairs of conventional 10× objectives were used as an objective and a condenser. Spectra were obtained through areas approximately 0.2 × 0.2 to 0.3 × 0.3 mm chosen to represent the clearest regions with the darkest and lightest pink color in the slab.

The intensity of the red color of the previously described Mn-rich tourmalines increased when they were irradiated with gamma rays (Reinitz and Rossman 1988). To determine if the Austrian Mn-rich olenite would respond in the same way to gamma ray irradiation, a pinkish-brown fragment was exposed to 50 Mrads of irradiation from ^{137}Cs at a rate of 0.87 Mrads per day from a sealed-source irradiator.

Synthesis experiments were designed to assess the correlation of Mn with Li, Al, and F in tourmaline over a temperature range from 550–750 °C at 200 MPa H_2O. Starting material was a reagent mix called "Syntur" that produces OH-dravite (Palmer et al. 1992), plus stepwise additions of Mn, Li, and F as added minerals or other reagents. In these experiments, the Li and Mn contents of the crystal-vapor assemblage were buffered by saturation in eucryptite (Li) or mica (Li + F) and in spessartine, rhodonite, or $MnBr_2$ (Mn) at the final stages of the experiments. Fluorine was added as AgF, which decomposed during the experiments to release F (and formed an MgF_2 precipitate in some experiments). Although Ag normally alloys with the Au of the capsule tube when the AgF decomposes, energy-dispersive X-ray analyses indicated that 1.5–2.0 wt% elemental Ag was incorporated into these homogeneous tourmaline crystals.

RESULTS AND DISCUSSION

Results

Optical absorption spectroscopy. Spectra (Fig. 1) are presented for a pink and a yellow-brown region of the crystal. In the **E⊥c** direction, a broad band near 530 nm is the dominant feature. Weaker broad bands appear centered near 710 and 1060

TABLE 1. Crystal data and results of structure refinement for Mn-rich tourmaline from Eibenstein an der Thaya, Lower Austria

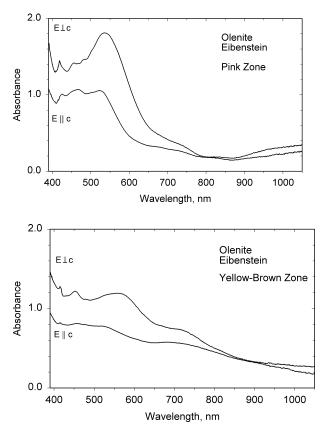| Space group	$R3m$	
Frame width, scan time, number of frames	0.20^0, 20 s, 4500	
Detector distance	5 cm	
Tourmaline sample:	BT	P6
Unit-cell parameters (Å)	a = 15.9466(3)	a = 15.941(1)
	c = 7.1384(3)	c = 7.136(1)
Reflections used in parameter refinement	9513	5681
Effective transmission	0.7571–1.0000	0.8425–1.0000
R_{int} (before-after SADABS)	0.040–0.030	0.047–0.022
Measured reflections, full sphere	10,164	10,334
Unique reflections; refined parameters	1113; 92	1119; 92
$R1, I > 4\sigma_I$	0.036	0.025
Difference peaks (e⁻/Å³)	+0.75(13), −0.71(13)	+0.96(10), −0.37(10)
Goodness-of-Fit	1.27	1.10

FIGURE 1. Optical absorption spectra of a single crystal fragment of Mn-rich olenite (NewBT) from Eibenstein an der Thaya, Austria, taken (**a**) in the deepest pink zone and (**b**) in the least pink zone. The two polarizations, obtained on a 0.245 mm thick slab, show both Mn^{2+} and Mn^{3+} features.

nm. All of these features are observed in the **E**‖**c** direction, but are of generally lower intensity. The spectra resemble previously published spectra of Mn-containing elbaites. The narrow bands near 415 nm have been assigned to Mn^{2+}, and most of the other bands have been assigned to Mn^{3+} (Reinitz and Rossman 1988). The exceptions are the bands near 1060 and 710 nm that are associated with Fe^{2+} (Mattson and Rossman 1987). The 710 nm Fe^{2+} band overlaps a Mn^{3+} band in the same region. Qualitatively, the spectra show that Mn^{2+} is present in all regions of the crystal, and that there is more Mn^{3+} in the pink regions than in the yellow-brown regions. The color of the sample is caused by a blend of Mn^{3+} features in the middle of the visible spectrum and the Mn^{2+} features that are more important in the short wavelength region of the spectrum. In the pink regions, the Mn^{3+} features dominate the spectrum and are the primary cause of color.

No absolute calibration exists for the intensity of Mn absorption bands in olenite. An attempt to determine the ratio of Mn^{3+} to total Mn was made using the molar absorptivity values reported for elbaite in Reinitz and Rossman (1988). Such values indicate that 8.2% of the total Mn is Mn^{3+} in the pink region of this Mn-rich olenite from Eibenstein and der Thaya, Austria. Because it is very difficult to determine the absolute intensity of the Mn^{2+} band that is superimposed on other bands

and the UV tail, it is unlikely that this is more than a semi-quantitative estimate. The uncertainty of the estimation is further emphasized when it is realized that the total Mn content was overestimated by nearly a factor of three. Even with these uncertainties, it appears that Mn^{2+} is the dominant oxidation state of this sample.

Irradiation experiment. The gamma-ray irradiated crystal fragment was distinctly pink compared to the yellow-brown color of the sample before irradiation, but it still had hints of the yellow-brown color. It was dichroic pink (**E** perpendicular to **c**) to pale pinkish-amber (**E**‖**c**). In a previously unreported experiment, Rossman and Mattson irradiated a brownish-yellow Zambian manganian-elbaite (GRR757) and observed that it was still brownish-yellow after 14 Mrads, but became pink admixed with yellow after 50 Mrads and just pink after 139 Mrads. In the experiments with the Zambian elbaite and tourmalines (Reinitz and Rossman 1988), during the course of the irradiation the intensity of the Mn^{2+} absorption bands near 412 nm decreased and the intensity of the broad absorption band near 580 nm assigned to Mn^{3+} increased. This experiment suggests that, like other Mn-bearing tourmalines, the natural pink color in the Eibenstein sample is due to natural irradiation of the initial Mn^{2+}.

Crystal structure. Refined cell-parameters and other crystal data of the Mn-rich tourmaline samples (BT, P6) are listed in Table 1. In Table 2, we list the atom parameters, and in Table 3, we present selected interatomic distances. Using quadratic programming methods, Wright et al. (2000) offer a method of optimizing the site occupancies of cation sites in minerals with multiply occupied cation sites; the optimized formula essentially minimizes the differences between the formula obtained from the results of the chemical analysis and that obtained by structure refinement. Using this method with the structure refinement and chemical data (Table 4) obtained in this study yields the structural formulae:

$$BT = {}^X(Na_{0.80}Ca_{0.01}\square_{0.19}) \; {}^Y(Al_{1.28}Mn^{2+}_{1.21}Li_{0.37}Fe^{2+}_{0.02}\square_{0.12}) \; {}^ZAl_6 \; {}^T(Si_{5.80}Al_{0.20}) \; B_3O_{27} \, [(OH)_{3.25}F_{0.43}O_{0.32}]$$

$$P6 = {}^X(Na_{0.77}Ca_{0.03}\square_{0.20}) \; {}^Y(Al_{1.23}Mn^{2+}_{1.14}Li_{0.48}Fe^{2+}_{0.02}Ti_{0.01}\square_{0.12}) \; {}^ZAl_6 \; {}^T(Si_{5.83}Al_{0.17}) \, B_3O_{27} \, [(OH)_{3.33}F_{0.48}O_{0.19}]$$

Even though optical spectroscopy indicated that there is a minor component of Mn^{3+}, Mn^{2+} is used in the formulae above. The absolute uncertainty in the proportions of Mn^{3+} and Mn^{2+} is large, so it is impossible to accurately assign the true oxidation states of Mn. Furthermore, the oxidized manganese is present as a radiation-induced color center. Thus, the formulae above probably represent the composition of the tourmaline at the time of formation (before ~336 Ma; Ertl et al. in preparation). We will use these formulae in later discussions of the atomic arrangements.

Discussion of the atomic arrangement

During refinement no significant change of the scattering value was observed when the occupancy of the T site was refined. Furthermore, the <T-O> distances (Table 3) are significantly enlarged relative to a site fully occupied with Si (1.620

TABLE 2. Atomic positions equivalent isotropic U for atoms in Mn-rich tourmaline

Atom	x	y	z	U_{eq}	Occ.
X					
BT	0	0	0.25	0.0276(19)	$Na_{0.82(2)}$
P6	0	0	0.25	0.0275(12)	$Na_{0.837(15)}$
Y					
BT	0.12442(10)	1/2x	–0.3585(8)	0.0113(4)	$Al_{1.248(11)}$
P6	0.12450(6)	1/2x	–0.3575(5)	0.0123(3)	$Al_{1.222(7)}$
Z					
BT	0.29797(8)	0.26132(8)	–0.3702(8)	0.0065(2)	$Al_{1.00}$
P6	0.29808(5)	0.26132(5)	–0.3695(5)	0.00786(14)	$Al_{1.00}$
T					
BT	0.19196(6)	0.19011(7)	0.0178(8)	0.00540(18)	$Si_{1.00}$
P6	0.19192(4)	0.19000(4)	0.0188(5)	0.00680(13)	$Si_{1.00}$
B					
BT	0.1100(2)	2x	0.4707(11)	0.0103(9)	$B_{1.00}$
P6	0.11015(13)	2x	0.4734(7)	0.0092(5)	$B_{1.00}$
O1					
BT	0	0	–0.2007(14)	0.046(3)	$O_{1.00}$
P6	0	0	–0.2000(8)	0.0487(18)	$O_{1.00}$
O2					
BT	0.06171(15)	2x	0.4976(10)	0.0226(10)	$O_{1.00}$
P6	0.06142(9)	2x	0.5004(6)	0.0231(6)	$O_{1.00}$
O3					
BT	0.2689(3)	1/2x	–0.4716(9)	0.0121(7)	$O_{1.00}$
P6	0.2687(2)	1/2x	–0.4710(6)	0.0129(4)	$O_{1.00}$
O4					
BT	0.09324(14)	2x	0.0884(9)	0.0106(7)	$O_{1.00}$
P6	0.09329(9)	2x	0.0887(5)	0.0108(4)	$O_{1.00}$
O5					
BT	0.1874(3)	1/2x	0.1111(9)	0.0097(6)	$O_{1.00}$
P6	0.18715(18)	1/2x	0.1110(5)	0.0111(4)	$O_{1.00}$
O6					
BT	0.19796(18)	0.18771(18)	–0.2072(9)	0.0093(5)	$O_{1.00}$
P6	0.19761(11)	0.18748(11)	–0.2059(5)	0.0101(3)	$O_{1.00}$
O7					
BT	0.28540(18)	0.28610(17)	0.0985(9)	0.0074(4)	$O_{1.00}$
P6	0.28546(11)	0.28588(10)	0.0990(5)	0.0088(3)	$O_{1.00}$
O8					
BT	0.21028(19)	0.2711(2)	0.4591(9)	0.0099(5)	$O_{1.00}$
P6	0.21016(12)	0.27115(12)	0.4602(5)	0.0109(3)	$O_{1.00}$
H3					
BT	0.268(6)	1/2x	0.439(11)	0.012(18)	$H_{1.00}$
P6	0.271(5)	1/2x	0.418(10)	0.06(2)	$H_{1.00}$

TABLE 3. Selected interatomic distances (Å) in Mn-rich tourmaline from Eibenstein an der Thaya, Lower Austria

X-	BT	P6
O2 ×3	2.456(6)	2.464(4)
O5 ×3	2.771(4)	2.768(3)
O4 ×3	2.822(4)	2.821(3)
Mean	2.683	2.684
Y-	BT	P6
O2 ×2	1.996(3)	1.986(2)
O6 ×2	2.049(3)	2.046(2)
O1	2.055(5)	2.054(3)
O3	2.153(5)	2.149(3)
Mean	2.050	2.045
Z-	BT	P6
O6	1.845(3)	1.852(2)
O8	1.877(3)	1.878(2)
O7	1.878(3)	1.880(2)
O8'	1.919(3)	1.920(2)
O7'	1.955(3)	1.954(2)
O3	1.973(2)	1.973(1)
Mean	1.908	1.910
T-	BT	P6
O6	1.610(3)	1.608(2)
O7	1.617(2)	1.615(2)
O4	1.626(2)	1.624(9)
O5	1.643(2)	1.639(1)
Mean	1.624	1.622
B-	BT	P6
O2	1.349(7)	1.359(4)
O8 ×2	1.387(4)	1.384(2)
Mean	1.374	1.376

Å; Hawthorne 1996; Ertl et al. 2001), and the chemical analyses (Table 4) show B ~ 3.0 apfu. Therefore no significant amounts of $^{[4]}B$ occur in these Mn-rich tourmaline samples from Austria. Refinement of the occupancy of the Z site showed that it is fully occupied with Al. Thus the occupancy at the Z site was fixed at $Al_{1.00}$ during the final stages of the refinements. The relationship between <T-O> distances and Al occupancy in the ring was first defined by Foit and Rosenberg (1979) and Foit (1989). MacDonald and Hawthorne (1995) showed with crystal structure analyses in combination with chemical analyses that very Mg-rich (and V-bearing) tourmaline samples can contain significant amounts of $^{[4]}Al$ (<T-O> = 1.627 Å for samples with 0.38–0.49 apfu $^{[4]}Al$). Prowatke et al. (2003) have shown by chemical analyses (including light elements) in combination with crystal structure determination that Mn-rich tourmaline from this Austrian locality can also contain significant amounts of $^{[4]}Al$, but no $^{[4]}B$ (0.33 apfu $^{[4]}Al$, <T-O> = 1.626 Å). The optimized formulae also show small amounts of $^{[4]}Al$ in these very Mn-rich tourmalines (optimized formula: 0.17–0.20 apfu $^{[4]}Al$; Table 4). This is in good agreement with the observed <T-O> distances of 1.622–1.624 Å (Table 3). Theses values are very similar to the calculated <T-O> distances of 1.622–1.623 Å by application of formula 1 from Ertl et al.

(2001). Table 5 shows the relationship between lattice parameters, MnO content, apfu Mn, and refined Al at the Y site in Mn-rich tourmalines.

No simple correlation exists between Mn content and <Y-O> distances, mainly because of different Li ~ Al substitutions in the samples listed in Table 5 (Li also enlarges the <Y-O> distance compared to Al). The <Y-O> distances of Mn-rich tourmaline from Austria in the range 2.045–2.050 Å are similar to <Y-O> distances of Fe- and Mg-rich tourmaline. The BeO content is very low (Table 4), and decreases as Mn increases: MnO ~ 5 wt%, BeO = 10 ppm (Prowatke et al. 2003); MnO ~ 8 wt%, BeO = 4 ppm (sample P6); MnO ~ 9 wt%, BeO = 1.5 ppm (sample BT).

As the optimized formulae of the Mn-rich tourmaline samples from Austria have an Al-dominated and not a Mn-dominated Y site, there is no need for a new name for these tourmaline samples. Because of the relatively high Al content and the low Li content (Al > Mn >> Li) at the Y site (26–32 mol% elbaite; a similar Li_2O content is seen in the rim of olenite from the type locality: 0.70 wt% Li_2O; Schreyer et al. 2002), these tourmaline samples are thus termed Mn-rich Li-bearing olenite. The SIMS values of Li_2O (Table 4) are similar to the value of 0.64 wt% Li_2O (by AAS) for an Mn-rich tourmaline sample from Zambia, described by Schmetzer and Bank (1984).

Combining our data with that of Tindle et al. (2002) (Figs. 7 and 18b of that work) and Prowatke et al. (2003), the Li content in natural tourmaline samples increases strongly (up to ~1 apfu Li) as the Mn content increases up to ~0.2 apfu Mn. As the Mn content increases further, up to ~0.4 apfu Mn, the Li content increases only slightly up to ~1.0–1.2 apfu Li. Above ~0.5 apfu Mn the Li content decreases to ~0.4 apfu Li for natu-

TABLE 4. Composition of Mn-rich tourmaline from Eibenstein an der Thaya, Lower Austria (wt%)

	BT*‡	BT§	P6†‡	P6§
SiO_2	35.28	35.31	35.52	35.59
TiO_2	0.02	0.02	0.05	0.05
B_2O_3	10.45	10.58	10.61	10.62
Al_2O_3	36.93	38.64	37.90	38.39
FeO#	0.15	0.15	0.14	0.14
MnO#	8.66	8.71	8.18	8.23
MgO	0.01	0.01	0.01	0.01
CaO	0.06	0.06	0.18	0.18
Li_2O	0.56	0.56	0.73	0.73
ZnO	0.00	–	0.02	0.02
Na_2O	2.13	2.51	2.64	2.43
K_2O	0.01	0.01	0.02	0.02
F	0.81	0.82	1.13	0.93
H_2O	2.88	2.97	3.04	3.05
O=F	–0.34	–0.35	–0.48	–0.39
Sum	97.61	100.00	99.69	100.00
N	31	31	31	31
Si	5.93	5.78	5.83	5.83
[4]Al	0.07	0.20	0.17	0.17
Sum T site	6.00	6.00	6.00	6.00
[3]B	3.03	3.00	3.01	3.00
Al	7.24	7.28	7.17	7.23
Mn^{2+}	1.23	1.21	1.14	1.14
Fe^{2+}	0.02	0.02	0.02	0.02
Mg	0.00	0.00	0.00	0.00
Zn	0.00	–	0.00	0.00
Ti	0.00	0.00	0.01	0.01
Li	0.38	0.37	0.48	0.48
Sum Y, Z sites	8.87	8.88	8.82	8.88
Ca	0.01	0.01	0.03	0.03
Na	0.69	0.80	0.84	0.77
K	0.00	0.00	0.00	0.00
Sum X site	0.70	0.81	0.87	0.80
Sum cations	18.60	18.69	18.70	18.68
H	3.23	3.25	3.33	3.33
F	0.43	0.43	0.59	0.48
Sum OH + F	3.66	3.68	3.92	3.81

* Average of 4 EMP analyses.
† Average of 10 EMP analyses.
‡ Average of 3 SIMS analyses for B_2O_3, Li_2O, and BeO and average of 2 SIMS analyses for H_2O. For sample BT BeO = 1.5 ppm, and for sample P6 BeO = 4 ppm.
§ Weight percent calculated from optimal site occupancies and normalized to 100%.
# Total Mn and total Fe calculated as MnO (see text) and FeO. Cl is below the detection limit in both samples.

ral tourmaline with ~1.2 apfu Mn (sample BT, this study). Indeed, experiments show that Mn-rich synthetic tourmaline is aluminous and Li is not essential for crystallization.

Possibly, because of the crystal chemical similarities of Mn^{2+} and Fe^{2+} and the fact that schorl samples can contain up to ~1.8 apfu Fe^{2+} (Grice and Ercit 1993), future tourmaline samples will be found with similar Mn contents. Relative to elbaite, when Mn increases in concentration, Al and Li decrease at the Y site. Our suggested short-range order configuration, (Mn^{2+}_2Al) at the Y site (Table 6) with ~50 mol% in the Mn-richest sample (BT), is a possible end-member occupation (see Hawthorne and Henry 1999) which may occur in nature.

For tourmaline samples with relatively high Mn contents and a significant Li-component the name Mn-rich elbaite was used previously, although Li was only calculated by previous authors (e.g., Shigley et al. 1986; Burns et al. 1994). Only tourmaline samples where the Mn-component > olenite-component

> elbaite-component at the Y site could properly be described as a new Mn-dominant member of the tourmaline group, as yet to be discovered. The *a* parameter in Mn-rich tourmalines (MnO: ≥ 3 wt%) is largely a function of the occupants at the Y site ($r^2 = 0.97$) (Fig. 2). The relationship between lattice parameter *a* and apfu Mn (Fig. 3; $r^2 = 0.91$) is not as good as for the refined Al value because of a variable Li and Al content at the Y site. Combining our structural and chemical data and by using these relationships (Fig. 2, Fig. 3) an Mn-rich (and Fe-poor) tourmaline with an Mn-dominated Y site (Mn > Al > Li) will probably have ≥16 e⁻ (by refinement) at the Y site and $a ≥ 15.97$ Å.

Relations to synthetic Mn-tourmaline

In a study of tourmaline from the Little Three pegmatite, Ramona, California, Morgan and London (1999) first identified a continuous and systematic variation from the schorl-olenite-foitite solid solution ("SOFTur": London 1999) that typifies tourmaline in granitic systems (London and Manning 1995; London 1999) to Mn-rich elbaite where tourmaline crystals project into miarolitic cavities (Mn-rich tourmaline crystals from Eibenstein an der Thaya occur intergrown with albite but not in miarolitic cavities). Though Li was not analyzed explicitly, the elbaite component was assessed through two compositional parameters derived from electron microprobe analyses: (1) the ratio of Al at the Y site to the sum of all Y cations, and (2) the parameter $Al^Y – \square^X$. In method 1, the elbaite component could be identified by the extent to which measurable occupancy at the Y site (excluding Li, which is not measurable by electron beam methods) decreased from a theoretical maximum of 3 apfu in SOFTur solid solutions (London and Manning 1995). In method 2, the operator $Al^Y – \square^X$ subtracts the component of foitite associated with Al at the Y site, though not the olenite component. Using these methods as measures of the elbaite component, tourmaline from the Little Three pegmatite showed a positive correlation of Mn with elbaite in the ratio 1:1. Starting with the schorl end-member, which represented a dominant component in the first-formed tourmaline, Morgan and London (1999) proposed the exchange vector (from schorl) of $MnLiAlFe_{-3}$. The natural solid solutions terminated
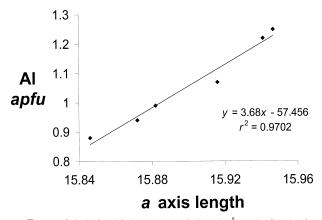

FIGURE 2. Relationship between *a* axis length (Å) and refined apfu Al from structural data at the Y site in Mn-rich, Fe-poor tourmaline samples (Table 5).

TABLE 5. Relation between lattice parameters, refined Al at the Y site (from structural data), MnO content, and apfu Mn (from chemical analyses) of Mn-rich tourmaline samples

a (Å)	c (Å)	Refined Al at the Y site	<Y-O> (Å)	MnO (wt%)	Mn (apfu)	Reference
15.846(3)	7.119(1)	0.88	2.019	3.07	0.41	Grice and Ercit (1993)
15.872(2)	7.138(4)	0.94	2.040	5.80	0.81	Burns et al. (1994), T10
15.882(7)	7.123(5)	0.99	2.036	5.99	0.84	Burns et al. (1994), T11
15.916(3)	7.130(1)	1.07	2.040	6.72	0.93	Nuber and Schmetzer (1984)
15.941(1)	7.136(1)	1.22	2.045	8.18	1.14	This work (sample P6)
15.9466(3)	7.1384(3)	1.25	2.050	8.66	1.23	This work (sample BT)

Note: The FeO content of all these samples is in the range 0.01–0.15 wt% FeO (0.00–0.36 wt% TiO_2, MgO at the detection limit). All these tourmaline samples have a Na-rich X site (0.66–0.85 apfu Na), and very low Ca contents (0.01–0.06 apfu Ca).

TABLE 6. Possible short-range order configurations in Mn-rich tourmaline (sample BT) from Eibenstein an der Thaya, lower Austria

Proportion	X site	Y site	T site	O1
0.33	Na	$Mn_2^{2+}Al$	Si_6	O
0.18	Na	$Mn_2^{2+}Al$	Si_5Al	OH
0.18	Na	$AlMn^{2+}Li$	Si_6	F
0.02	Na	Al_2Fe^{2+}	Si_5Al	O
0.09	Na	$Al_2\square$	Si_6	OH
0.01	Ca	$Al_2\square$	Si_6	O
0.19	$\square$	Al_2Li	Si_6	F

Calculated occupants:
X = $(Na_{0.80}Ca_{0.01}\square_{0.19})$ Y = $(Al_{1.31}Mn_{1.20}^{2+}Li_{0.37}Fe_{0.02}^{2+}\square_{0.10})$ T = $(Si_{5.80}Al_{0.20})$ O1 = $[F_{0.37}(OH)_{0.27}O_{0.36}]$ O3 = $(OH)_3$
Optimized occupants:
X = $(Na_{0.80}Ca_{0.01}\square_{0.19})$ Y = $(Al_{1.28}Mn_{1.21}^{2+}Li_{0.37}Fe_{0.02}^{2+}\square_{0.12})$ T = $(Si_{5.80}Al_{0.20})$ O1 = $[F_{0.43}(OH)_{0.25}O_{0.32}]$ O3 = $(OH)_3$
Note: O3 = $(OH)_3$ for all short range order configurations.

FIGURE 4. Backscattered electron image of a typical synthetic Mn-rich tourmaline (OH-rich dravite euhedra) plus albite experimental product.
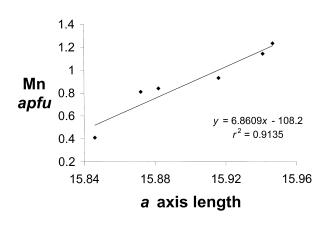

FIGURE 3. Relationship between a axis length (Å) and apfu Mn (from chemical analyses) in Mn-rich, Fe-poor tourmaline samples (Table 5).

at ~1 Mn apfu and ~1 LiAl apfu— the theoretical limit for this substitution (Fig. 5f in Morgan and London 1999). The fluorine content of tourmaline also correlated positively with Mn and with the calculated elbaite component.

With these observations from natural tourmaline, we began a series of experiments designed to assess the correlation of Mn with Li, Al, and F in tourmaline (experimental details listed previously). Preliminary results of this work are cited in London et al. (2001) and are explained further here. The resultant tourmaline of these experiments forms fine-grained but homogeneous radial crystal sprays (Fig. 4). The Mn content of tourmaline appears to increase with decreasing temperature (Fig.
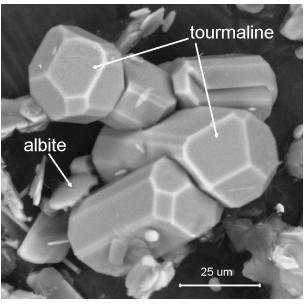
5), though this correlation is poor on the basis of existing experimental results (in Fig. 5, N = total number of microprobe data points). There is a weak positive correlation between Mn and Al at the Y site (9b) of tourmaline (Fig. 6), though the correlation is even poorer than in Figure 5, and the linear regression is dominated by a positive correlation seen in experiments at 650 °C. Neither fit improves when the data are segregated on the basis of starting composition (i.e., Syntur + Mn, + Mn + F, + Mn + Li, or + Mn + F + Li). Finally, there is essentially no correlation between the Mn and Li contents of tourmaline in these experiments. Figure 7 shows Li* (Li* = Li calculated by difference to three atoms at the Y site; Selway and Xiong, personal communication, 2002) vs. Mn for experiments containing Syntur + Mn + Li + F. Though many experiments were saturated with crystalline Li-rich phases (mica or eucryptite) the average Li* content of all tourmaline (in 203 analyses from Li + Mn-bearing systems) was only 0.05 Li* apfu over the range of 550–750 °C.

In conclusion, though a strong positive correlation exists between Mn and Li (elbaite) in tourmaline from the Little Three pegmatite, and also in tourmaline from petalite-subtype granitic pegmatites northwestern Ontario, Canada (Tindle et al.
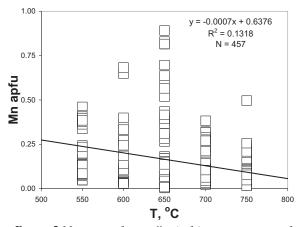
FIGURE 5. Mn content of tourmaline (apfu) versus temperature for all experiments that contained Mn in addition to Syntur (see text), Li, and/or F.
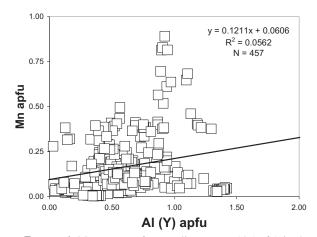

FIGURE 6. Mn content of tourmaline versus Al (apfu) in the octahedral Y site (9*b* site) for all experiments that contain Mn in addition to Syntur (see text), Li, and/or F.
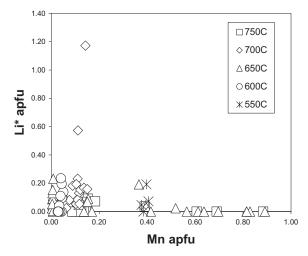

FIGURE 7. Mn content of tourmaline vs. Li* (apfu, calculated by the data reduction program of Selway and Xiong, personal communication, 2002) for all experiments between 550–750 °C that contain Syntur (see text) + Mn + Li + F.

2002; Mn contents up to ~0.4 apfu), this coupling is not required to promote compatibility of Mn in tourmaline. Like the tourmaline from Eibenstein an der Thaya, Mn-rich tourmaline in these experiments, containing up to ~0.9 apfu Mn (6.37 wt% MnO), is aluminous but not Li-rich.

REFERENCES CITED

Burns, P.C., MacDonald, D.J., and Hawthorne, F.C. (1994) The crystal chemistry of manganese-bearing elbaite. Canadian Mineralogist, 32, 31–41.
Duparc, L., Wunder, M., and Sabot, R. (1913) Die Mineralien der Pegmatite in der Umgebung von Antsirabé auf Madagascar. Zeitschrift für Kristallographie, 52, 294–300.
Dyar, M.D., Taylor, M.E., Lutz, T.M., Francis, C.A., Guidotti, C.V., and Wise, M. (1998) Inclusive chemical characterization of tourmaline: Mössbauer study of Fe valence and site occupancy. American Mineralogist, 83, 848–864.
Dyar, M.D., Wiedenbeck, M., Robertson, D., Cross, LR., Delaney, J.S., Ferguson, K., Francis, C.A., Grew, E.S., Guidotti, C.V., Hervig, R.L., Hughes, J.M., Husler, J., Leeman, W., McGuire, A.V., Rhede, D., Rothe, H., Paul, R.L., Richards, I., and Yates, M. (2001) Reference Minerals for the Microanalysis of Light Elements. Geostandards Newsletter, 25, 441–463.
Ertl, A., Hughes, J.M., and Marler, B. (2001) Empirical formulae for the calculation of <T-O> and X-O2 bond lengths in tourmaline and relations to tetrahedrally-coordinated boron. Neues Jahrbuch Mineralogie Monatshefte, 12, 548–557.
Foit, F.F., Jr. (1989) Crystal chemistry of alkali-deficient schorl and tourmaline structural relationships. American Mineralogist, 74, 422–431.
Foit, F.F., Jr. and Rosenberg, P.E. (1979) The structure of vanadium-bearing tourmaline and its implications regarding tourmaline solid solutions. American Mineralogist, 64, 788–798.
Grice, J.D. and Ercit, T.S. (1993) Ordering of Fe and Mg in the tourmaline crystal structure: The correct formula. Neues Jahrbuch Mineralogie Monatshefte, 165, 245–266.
Hawthorne, F. C. (1996) Structural mechanisms for light-element variations in tourmaline. Canadian Mineralogist, 34, 123–132.
Hawthorne, F.C. and Henry, D.J. (1999) Classification of the minerals of the tourmaline group. European Journal of Mineralogy, 11, 201–215.
Kalt, A., Schreyer, W., Ludwig, T., Prowatke, S., Bernhardt, H.-J., and Ertl, A. (2001) Complete solid solution between magnesian schorl and lithian excess-boron olenite in a pegmatite from Koralpe (eastern Alps, Austria). European Journal of Mineralogy, 13, 1191–1205.
King, P.L., Vennemmann, T.W., Holloway, J.R., Hervig, R.L., Lowenstern, J.B., and Forneris, J.F. (2002) Analytical techniques for volatiles: A case study using intermidiate (andesitic) glasses. American Mineralogist, 87, 1077–1089.
Kunitz, W. (1929) Die Mischungsreihen in der Turmalingruppe und die genetischen Beziehungen zwischen Turmalinen und Glimmern. Chemie der Erde, 4, 208–251.
London, D. (1999) Stability of tourmaline in peraluminous granite systems: the boron cycle from anatexis to hydrothermal aureoles. European Journal of Mineralogy, 11, 253–262.
London, D. and Manning, D.A.C. (1995) Compositional variation and significance of tourmaline from southwest England. Economic Geology, 90, 495–519.
London, D., Evensen, J.M., Fritz, E., Icenhower, J.P., Morgan, G.B. VI, and Wolf, M.B. (2001) Enrichment and accommodation of manganese in granite-pegmatite systems. 11th Annual Goldschmidt Conference Abstract 3369, Lunar Planetary Institute Contribution 1088, Lunar Planetary Institute, Houston (CD-ROM).
MacDonald, D.J. and Hawthorne, F.C. (1995) The crystal chemistry of Si ↔ Al substitution in tourmaline. Canadian Mineralogist, 33, 849–858.
Mattson, S.M. and Rossman, G.R. (1987) Fe^{2+}-Fe^{3+} interactions in tourmaline. Physics and Chemistry of Minerals, 14, 163–171.
Morgan, G.B. VI and London, D. (1999) Crystallization of the Little Three layered pegmatite-aplite dike, Ramona District, California. Contributions to Mineralogy and Petrology, 136, 310–330.
Novák, M. (2000) Compositional pathways of tourmaline evolution during primary (magmatic) crystallization in complex (Li) pegmatites of the Moldanubicum, Czech Republic. Memorie della Società Italiana di Science Naturali e del Museo Civico di Storia naturale di Milano, 30, 45–56.
Nuber, B. and Schmetzer, K. (1984) Structural refinement of tsilaisite (manganese

tourmaline). Neues Jahrbuch für Mineralogie, Monatshefte, 1984, 301–304.

Ottolini, L., Bottazzi, P., and Vannucci, R. (1993) Quantification of lithium, beryllium, and boron in silicates by secondary Ion Mass Spectrometry using conventional energy filtering. Analytical Chemistry, 65, 1960–1968.

Palmer, M.R., London, D., Morgan, G.B., VI, and Babb, H.A. (1992) Experimental determination of fractionation of $^{11}B/^{10}B$ between tourmaline and aqueous vapor: A temperature- and pressure-dependent isotopic system. Chemical Geology, 101, 123–129.

Perkins, W.T., Pearce, N.J.G., and Westgate, J.A. (1997) The development of laser ablation ICP-MS and calibration strategies; examples from the analyses of trace elements in volcanic glass shards and sulfide minerals. Geostandards Newsletter, 21, 115–144.

Prowatke, S., Ertl, A., and Hughes, J.M. (2003) Tetrahedrally-coordinated Al in Mn-rich, Li- and Fe-bearing olenite from Eibenstein an der Thaya, Lower Austria: A chemical and structural investigation. Neues Jahrbuch Mineralogie Monatshefte, 2003, 385–395.

Reinitz, I.L. and Rossman, G.R. (1988) Role of natural radiation in tourmaline coloration. American Mineralogist, 73, 822–825.

Rossman, G.R. and Mattson, S.M. (1986) Yellow, Mn-rich elbaite with Mn-Ti intervalence charge transfer. American Mineralogist, 71, 599–602.

Schmetzer, K. and Bank, H. (1984) Crystal chemistry of tsilaisite (manganese tourmaline) from Zambia. Neues Jahrbuch für Mineralogie Monatshefte, 1984, 61–69.

Schreyer, W., Hughes, J.M., Bernhardt, H.-J., Kalt, A., Prowatke, S., and Ertl, A. (2002) Reexamination of olenite from the type locality: detection of boron in tetrahedral coordination. European Journal of Mineralogy, 14, 935–942.

Shigley, J.E., Kane, R.E., and Manson, D.V. (1986) A notable Mn-rich gem elbaite tourmaline and its relationship to "tsilaisite". American Mineralogist, 71, 1214–1216.

Tindle, A.G., Breaks, F.W., and Selway, J.B. (2002) Tourmaline in petalite-subtype granitic pegmatites: evidence of fractionation and contamination from the Pakeagama Lake and Separation Lake areas of northwestern Ontario, Canada. Canadian Mineralogist, 40, 753–788.

Wright, S.E., Foley, J.A., and Hughes, J.M. (2000) Optimization of site occupancies in minerals using quadratic programming. American Mineralogist, 85, 524–531.